Remote Sensing Based Land Cover Map of Watersheds in the Swedish Arctics: Study of Spatial and Temporal Variabilities of Land Cover

Yves AUDA Auda * , Erik J. Lundin , David Gustafsson , Oleg S. Pokrovsky , Simon Cazaurang , Laurent Orgogozo

Posted Date: 20 April 2023

doi: 10.20944/preprints202304.0653.v1

Keywords: land cover; sentinel-2 images; random forest; boreal forest; alpine tundra

Article

Remote Sensing Based Land Cover Map of Watersheds in the Swedish Arctics: Study of Spatial and Temporal Variabilities of Land Cover

Yves Auda [1,*], Erik J. Lundin [2], David Gustafson [2], Oleg S. Pokrovsky [1,3], Simon Cazaurang [4] and Laurent Ogogozo [2]

[1] GET (Géosciences Environnement Toulouse), UMR 5563 CNRS/UR 234 IRD/UPS, Observatoire Midi Pyrénées, Université de Toulouse, Toulouse, France
[2] Swedish Polar Research Secretariat, Abisko Scientific Research Station, Sweden
[3] BIO-GEO-CLIM Laboratory, Tomsk State University, Tomsk, Russian Federation
[4] Toulouse Institute of Fluid Mechanics (IMFT), National Polytechnic Institute of Toulouse, Toulouse, F-31400, France
* Correspondence: yves.auda@get.omp.eu; Tel.: +33(0)6 02 24 51 13

Abstract: A land cover map of two arctic catchments, nearby the Abisko Scientific Research Station, was obtained from a classification of a Sentinel-2 satellite image and a ground survey performed in July 2022. The two contiguous catchments, Miellajokka and Stordalen, are covered by various ecotypes, from boreal forest to alpine tundra and peatland. The Random Forest algorithm correctly identified 83% of polygon pixels reserved for testing. The developed workflow relied solely on open source software and acquired ground observations. Space organization was directed by the altitude as demonstrated by the intersection of the land cover with the topography. Comparison between this new land cover map and previous ones based on data acquired between 2008 and 2011 shows some trends of vegetation cover evolution in response to climate change in the considered area.

Keywords: land cover; sentinel-2 images; random forest; boreal forest; alpine tundra

1. Introduction

When it comes to hydrological and biogeochemical fluxes on continental surfaces, the nature of the land cover, including both vegetation covers, bare rock outcrops and surface water bodies is of major importance [1–3]. It is especially true in the Arctic, where permafrost conditions may strongly control the present ecotypes and their distributions [4–7], while vegetation cover variability may in turn significantly impact thermo-hydrological conditions through evapotranspiration for instance [8,9]. Thus permafrost modeling requires detailed knowledge of the land cover distribution.

The vast extension and the remoteness of the Arctic regions make the establishment of field survey – based land cover maps difficult. Moreover, high resolutions and open data maps are needed for many applications [10]. Thus there is a growing interest in airborne [11,12] and remote sensing [13–15] capable of producing high-resolution vegetation maps in the Arctics. These regions are experiencing intensive climate change [16]. Permafrost thawing results in methane emissions [17] which contributes to the greenhouse effect. These modifications induce changes in ecotypes [18] that are visible at the landscape level. Thus there is a need for not only high spatial resolution maps, but also for high temporal resolution survey. In order to produce regularly updated land cover map for large areas, the use of remote sensing data from long term satellite missions combined with in-situ information is required [14].

Here we present a workflow for making high resolution vegetation map using only open data and open source softwares along with dedicated field data. The workflow is applied to two watersheds in the Swedish Arctic, for parts of which previous vegetation maps at lower resolutions and/or in past climatic conditions where already available [11,19,20]. The obtained map is used for

Preprints (www.preprints.org) | NOT PEER-REVIEWED | Posted: 20 April 2023 doi:10.20944/preprints202304.0653.v1

studying link between topography and vegetation distribution, and also the temporal evolution of the vegetation cover during a 14 years period (2008-2022).

2. Materials and Methods

2.1. Field sites

Two watersheds close to Abisko Scientific Research Station are considered (Figure 1). The first one from West to East is Miellajokka, a sub-alpine catchment which include the iconic mounts of Tjuonavagge (Lapporten). This 51.5 km² catchment presents altitudes ranging from 383 to 1731 m above see level [21]. The most eastern watershed is Stordalen, a 16 km² catchment with a lake-rich, peat-rich Northern part, and a sub-alpine Southern part, with elevation between 350 and 770 m above see level [22–25]. In Stordalen vegetation maps of the Northern, low elevation part has been already produced with airborne data of 2000 [19]. Later on, another vegetation map for the whole watershed has been produced with airborne data of 2008 [20]. Both Stordalen and Miellajokka are encompassed in the area studied by Reese, with a vegetation map established on the basis of 2010 satellite images, using also data acquired by lidar survey [11].

Figure 1. Location of the study sites and the Abisko monitoring station.

2.2. Satellite data

Obtaining images in the Arctic zone to study vegetation cover is difficult. These geographical areas are covered with snow for a large part of the year, which prevents any satellite study of the vegetation cover. In addition, frequent clouds hinder the acquisition of optical images. A single Sentinel-2 image acquired on 25 August 2022 is downloaded from https://peps.cnes.fr. Ten bands were selected for land cover classification (Table 1). The image is not corrected for atmospheric effects (Level-1C). The images are stored in the UTM34N reference coordinate system and all calculations are performed in this system to avoid altering the radiometry by re-projection.

Table 1. Sentinel-2 bands selected for land cover classification.

Band	Resolution (m)
B02 - blue	10
B03 - green	10
B04 - red	10
B05 – red-edge 1	20
B06 – red-edge 2	20
B07 - red-edge 3	20
B08 - NIR	10
B08A – narrow NIR	20
B11 – SWIR 1	20

Preprints (www.preprints.org) | NOT PEER-REVIEWED | Posted: 20 April 2023 doi:10.20944/preprints202304.0653.v1

B12 – SWIR 2	20

On the basis of four (B03, B04, B08, B11) out of the ten acquired channels, four derived indices are calculated: Bright, NDVI, NDWI, NDII (Table 2). The bright index is very sensitive to albedo. It distinguishes between light and dark soils. The NDWI (Normalized Difference Water Index) was used to detect water areas. The NDVI expressed the photosynthesis of the vegetation cover. The use of NDII [26,27] did not improve the results and was not retained for the final classification.

Table 2. Vegetation indices. Band notation correspond to MSI sensor of sentinel-2 satellite.

Index	Formula
Bright	$\sqrt{(B04 * B04)/(B08 * B08)}$
NDVI	$(B08 - B04)/(B08 + B04)$
NDWI	$(B03 - B08)/(B03 + B08)$
NDII	$(B08 - B11)/(B08 + B11)$

Since vegetation in mountainous areas is related to altitude, the digital terrain model is a very useful data source. ArcticDEM is an NGA-NSF public-private initiative to automatically produce a high-resolution digital surface model of the Arctic using optical stereo imagery. The majority of ArcticDEM data was generated from the panchromatic bands of the WorldView-1, WorldView-2, and WorldView-3 satellites and, for a small percentage of data, from the GeoEye-1 satellite. For this study, ArticDEM Release 7 "mosaic" format files with a spatial resolution of 2 m are downloaded at https://data.pgc.umn.edu/elev/dem/setsm/ArcticDEM/mosaic/v3.0/.

2.3. Field survey

The field mission took place from 21 July 2022 to 24 July 2022 in the Miellajokka and Stordalen watersheds, northern Sweden. A "Samsung Galaxy Tab S6 Lite" tablet is used to perform the field surveys. It supports GPS, GLONASS, Beidou and Galileo navigation systems. The Qfield software is used for data entry in the field. Its compatibility with QGIS simplifies data collection and subsequent analysis [28].

A database including a color composite of Sentinel-2 image channels B08/B04/B03, the Open Street Map data and an empty vector layer intended for the field surveys is prepared in QGIS then transferred to Qfield. The surveys are made in the form of polygons drawn once in the field at the polygon locations with the pen of the tablet. Each polygon is associated with the observed land use class at the considered place, and possibly a photo is taken with the tablet camera. The land cover classes are initially defined from Reese [11]. However, the 270 surveys conducted during our mission only identified 7 classes (Table 3) out of the 12 classes of Reese. The rock class is mainly composed of fresh bed rock outcrops but it may also includes thin organic soil and sediment. The alpine meadow was not encountered enough during the field trip to constitute a class. Likewise, the Mountain birch - meadow type class was only encountered in 6 surveys and is grouped with the Mountain birch - moss type class to form a single Mountain birch class. Areas in snow that were very poorly represented, during the July mission, are not included. Grass heaths were not encountered. A new class, 'Human infrastructure', is added, representing mainly the road and the railway passing through the mapped area. Shadows in the steep areas to the south of the study area hinder recognition of the landscape they cover. To avoid confusion, especially with water, a shadow class is created, making the number of considered classes equaled to 9.

Table 3. Land cover classes.

Class
Rock
Dry heath
Mesic heath

Preprints (www.preprints.org) | NOT PEER-REVIEWED | Posted: 20 April 2023 doi:10.20944/preprints202304.0653.v1

Wetland
Alpine willow
Mountain birch
Water
Human infrastructure
Shadow

2.4. Classification

The Random Forest method [29] uses decision trees and random draws without replacement of samples and variables to classify the Sentinel-2 image. Within each class, 30% of the polygons are randomly drawn and reserved for classification quality assessment. The classification is trained with the remaining 70%. GRASS software is used for the calculations [30]. The extension r.learn.ml2 interfaces with the Scikit-learn library written in python to perform Random Forest classification.

3. Results

3.1. Vegetation map in current climatic conditions

The classified image (Figure 2) shows patterns consistent with the knowledge of the terrain. The transport infrastructures are described with precision in their continuity. The lake Torneträsk at the North is homogeneously identified.

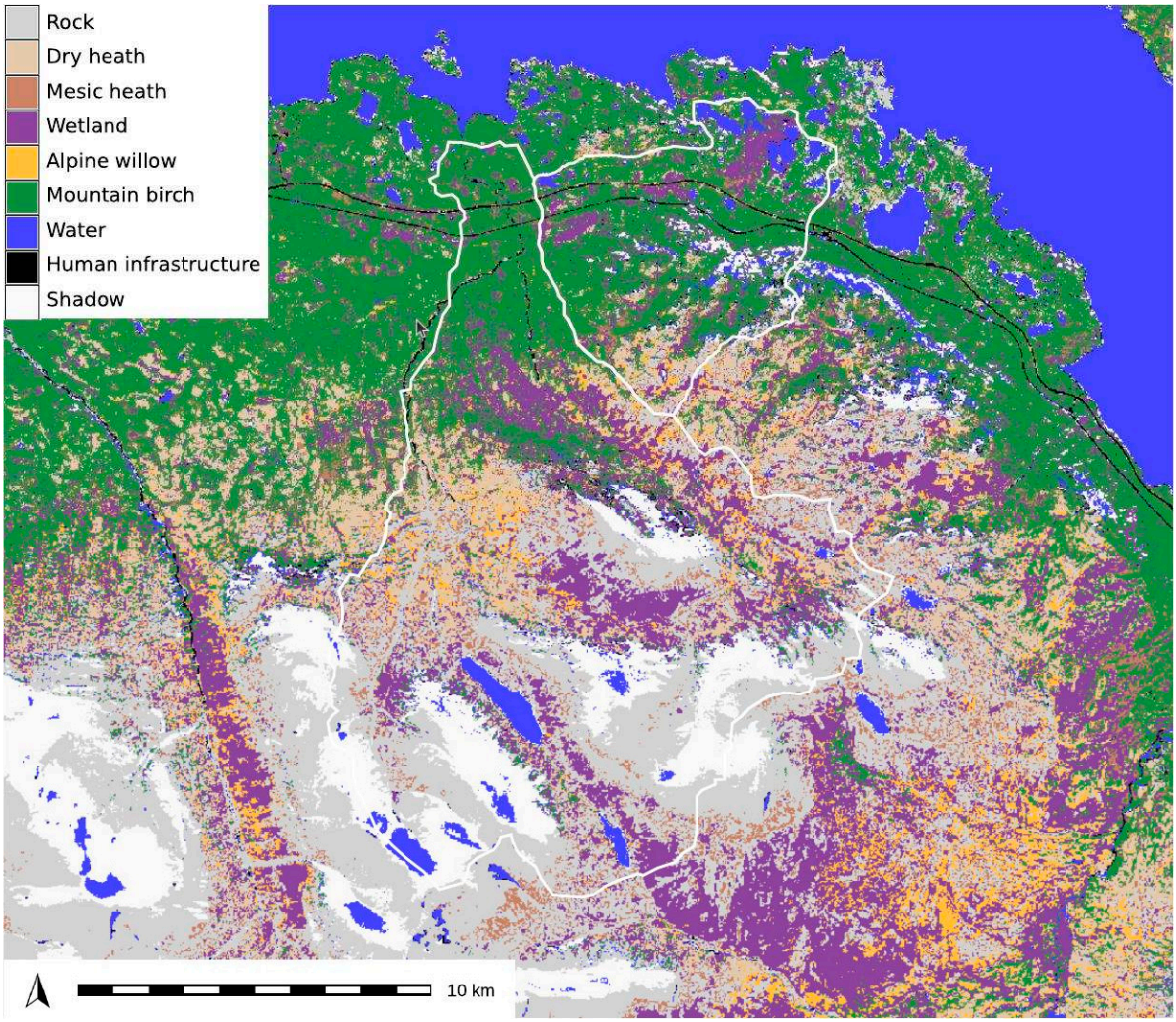

Figure 2. Image classified from the July 2022 field survey.

Preprints (www.preprints.org) | NOT PEER-REVIEWED | Posted: 20 April 2023 doi:10.20944/preprints202304.0653.v1

The statistics confirm the quality of the classification. The percentage of pixels correctly classified by Random Forest is 83%. The confusion matrix (Table 4) provides an analysis of the accuracy of the classification used for building our map at the class level. The columns show the field surveys and the rows show the classification results. For instance, the number 117 corresponds at the cross of the "mountain birch" line and the "mesic heath" column means that 117 pixels that have been classified as "mountain birch" belong to "mesic heath" according to the field survey. The largely dominant weight of the diagonal terms in this confusion matrix demonstrates the quality of the classification. The confusion between "Dry heath" and "Mesic heath" is understandable because these two formations are differentiated primarily by canopy height, a feature not accessible from the images used in our study. Likewise, the confusion between "Alpine willow" and "Wetland" is due to the difficulty of recognizing spaces occupied by a few willow plants. Besides, with such a pixel classification approach, places that are temporarily flooded at the moment of the satellite image acquisition are difficult to distinguished from true wetlands, i.e. places that are under water almost all along the active season. This could lead to overestimate the wetland area, including into it places with other vegetation types like meadow temporarily flooded by ground water discharge or snowmelt water. Another important point is the detection of temporary high elevation open water bodies in several places around Lapporten lake, according to both this classification and the two indices NDII, NDVI values of the pixels. These ones may be generated by late snowmelt in the highest places of the landscape. Finally, the confusion between "Dry heath", "Mesic heath" and "Mountain birch" are classes that can be contiguous and even associated in some places. It describes mixed spaces where several classes coexist, i.e. ecotone between these classes.

Table 4. Confusion matrix of the Random Forest classification. The asteriks highlights in confusion matrix indicates the most significant confusions.

	Rock	Dry heath	Mesic heath	Wetland	Alpine willow	Mountain birch	Water	Human infrastructure	Shadow
Rock	84	2	15	0	0	2	0	0	0
Dry heath	0	168	59*	11	18	2	0	0	0
Mesic heath	17	18	49	5	6	8	0	0	0
Wetland	0	0	0	484	51*	6	4	1	
Alpine willow	0	2	4	0	40	1	0	0	0
Mountain birch	0	98*	117*	102*	38*	1312	8	1	0
Water	2	0	0	1	0	0	2913	12	309
Human infrastructure	1	0	0	0	0	0	8	47	0
Shadow	5	0	0	0	0	0	44	10	2051

The "Mountain birch" class is the most represented (Table 5). It occupies more than a quarter of the space. The rock class and the wetlands ("Wetland" and "Alpine willow") share 40% of the spaces. The other classes are much smaller.

Table 5. Distribution of land cover classes of our classification. The shadow class is not taken in account.

Class	Percentage
Rock	21
Dry heath	9
Mesic heath	4

Preprints (www.preprints.org) | NOT PEER-REVIEWED | Posted: 20 April 2023 doi:10.20944/preprints202304.0653.v1

Wetland	16
Alpine willow	4
Mountain birch	29
Water	16
Human infrastructure	1

3.2. Influence of altitude on land cover

Land cover appears to be strongly conditioned by altitude. Altitudinal zonation of land cover is encountered in various arctic contexts [31–33], including in the Abisko region [34,35]. In Miellajokka catchment, the seasonal variability of the hydrogeochemistry of the stream indicates a strong altitudinal control on hydrological processes, especially during the spring freshet [36], while hydrological conditions strongly interact with vegetation and CO_2 fluxes [37]. Table 6, constructed by cross-referencing the land cover map with the ArticDEM, illustrates this phenomenon in the studied watersheds.

Table 6. Percentage of land cover classes according to altitudinal levels. The water, human infrastructure and shadow classes are not taken in account.

Land cover	Level class (m)			
	Subalpine < 600	Low alpine [600,800[	High alpine [800,1100[	Nival > 1100
Rock	2	4	33	88
Dry heath	3	19	16	0
Mesic heath	3	7	5	6
Wetland	11	24	30	6
Alpine willow	1	6	9	0
Mountain birch	80	40	7	0

The subalpine level at altitudes below 600 m is mainly occupied by the "Mountain birch" class. The Alpine stage includes the "Dry heath", "Mesic heath", "Wetland" and "Alpine willow" formations. It is divided into two sub-stages: Between 600 and 800 m of altitude, the "Mountain birch" class is still very present. Above 800 m, this class gives way to the rock. The nival stage is composed only of rock, probably because it depends on harsher life conditions and more intense erosive processes at higher elevations.

3.3. Comparison between past and present vegetation maps

Three maps of parts of our study area have been produced by different authors. A map was constructed from aerial images of 8 August 1970 and 29 July 2000 [19], but the area covered is too small to allow comparison with our data. Another map of the Stordalen watershed was obtained from images obtained from a helicopter flight on 1 August 2008 [23]. The most recent map of the Miellajokka watershed was produced from SPOT5 images of 28 July 2011 and laser data acquired under leaf-on conditions from two scanning dates (20 August 2010 and 9 September 2010) [11,38]. As the semantics of these maps are not identical to ours, an analysis of the variable typologies is necessary prior to the study of the landscape evolution. In order to overlay the maps and then calculate statistics, the Lundin and Reese maps extracted from the publications were georeferenced from control points identified in the landscape.

Comparison with the map of Reese

Reese [11,38] produced a land cover map with a larger number of classes. In order to compare the Reese map with our data, some classes of the Reese map are combined. "Snow ice" and "Snow bed" classes are grouped together. "Dry heath", "Extremely dry heath", "Grass heath" are also grouped together. The "Human infrastructure" class is not considered because it does not exist in

Preprints (www.preprints.org) | NOT PEER-REVIEWED | Posted: 20 April 2023 doi:10.20944/preprints202304.0653.v1

Reese's work. "Alpine meadow" and "Tall Alpine meadow" were not confirmed by ground observations during our field trip.

The spatial distribution of the classes is slightly different (Tables 7 and 8). The "Rock" class accounts for 36% for our classification and only 14% for the Reese map.

Table 7. Distribution of land cover classes of Reese [11] in the Miellajokka watershed.

Class	Percentage
Rock	14
Dry heath / Extremely dry heath / Grass heath	26
Mesic heath	4
Wetland	4
Alpine willow	19
Mountain birch	13
Water	4
Snow Ice, Snow bed	5
Alpine meadow / Tall alpine meadow	11

Table 8. Distribution of land cover classes of our classification in the Miellajokka watershed. The shadow class is not taken in account.

Class	Percentage
Rock	36
Dry heath	11
Mesic heath	5
Wetland	22
Alpine willow	4
Mountain birch	18
Water	4

The change matrix shown in Table 9 encompasses the differences in semantics of classes and the changes in the landscape between the dates of the two maps (i.e.: 2014 and 2022), and may be also discrepancies due to the use of different methodologies. Table 9 and Figure 3 show that some "Rock" areas in the middle our map are covered by "Grass heath", "Dry heath" and "Alpine willow" on the Reese map. The forest is also growing slightly to the south in sparse patches.

Table 9. Change matrix comparing our classification to the map [11]. Each column corresponds to the percentage of pixels of a class obtained by our classification in function of the Reese map classes. The shadow class is not taken in account.

		Our classification						
		Rock	Dry heath	Mesic heath	Wetland	Alpine willow	Mountain birch	Water
Reese map	Rock	32	3	10	3	2	1	12
	Dry heath / Extremely dry heath / Grass heath	32	36	41	24	33	8	9
	Mesic heath	1	4	3	5	6	10	1
	Wetland	2	6	3	7	9	3	1
	Alpine willow	15	29	22	24	31	14	10
	Mountain birch	0	4	8	12	7	53	1

Preprints (www.preprints.org) | NOT PEER-REVIEWED | Posted: 20 April 2023 doi:10.20944/preprints202304.0653.v1

Water	3	2	3	3	2	4	38
Snow Ice, Snow bed	8	2	2	2	1	1	24
Alpine meadow/Tall alpine meadow	7	14	8	20	9	6	4

On the other hand, "Alpine willow" is also more represented on Reese map without any conclusion being drawn because this class is misclassified by Reese [11]: the confusion matrix indicates 20 of 44 pixels misclassified. In addition, "Alpine meadow" which we have not taken into account, is identified as "Wetland" on our map (Figure 3), maybe because most of "Alpine meadow" places were temporarily flooded at the time of observation(see also Section 3.1). This class "Wetland" exists on the map published by Borgelt [38] but it is not present in the confusion matrix published by Reese [11]. The other classes do not show significant difference in in their proportion and spatial distribution.

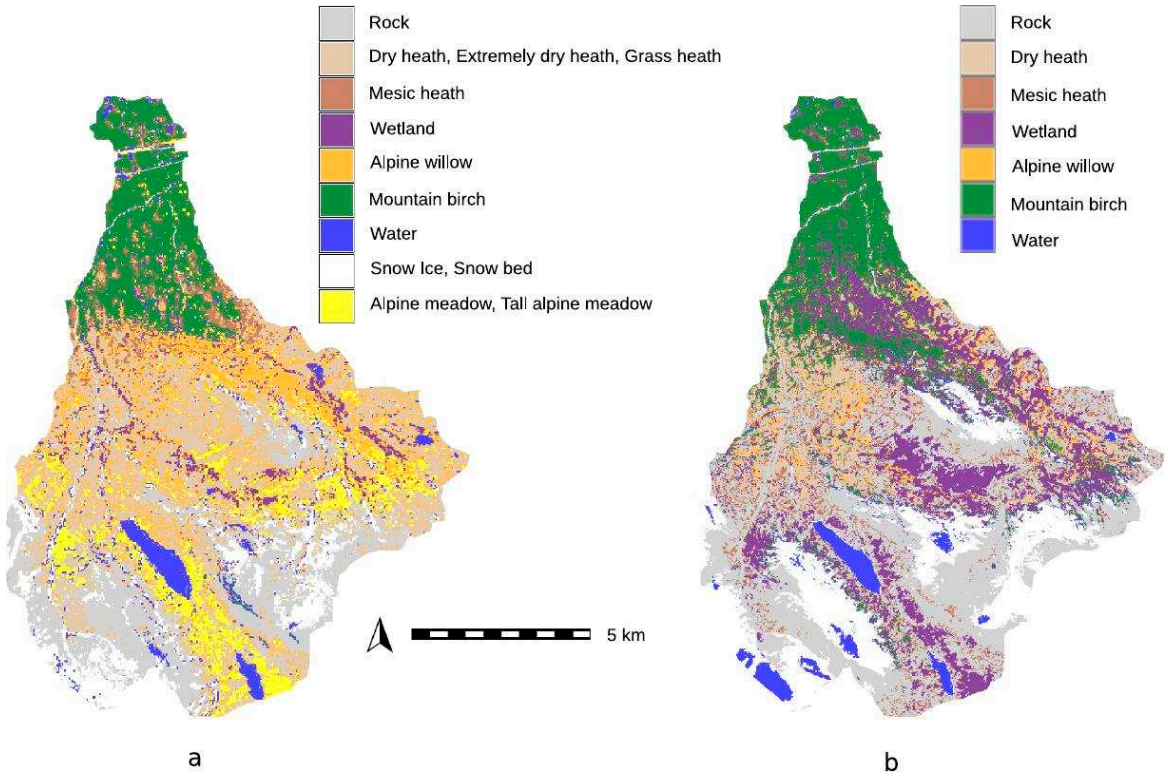

Figure 3. Land cover map by Reese [11] (a) and our reclassified map (2022) (b) in the Miellajokka watershed.

Despite the differences between the two maps, Figure 3 shows a great consistency in the distribution of space. Three elements can explain these differences. 1) The landscape is natural. There are no parcels to structure it. Between areas occupied by two vegetation classes there is often a transition zone which is difficult to assign to a class. 2) The class definition of Reese [11] takes into account the height of the stratum using metrics derived from laser acquisitions, a technology we did not employ. 3) The landscape has evolved between 2010 and 2022. For example, some areas of rock have become vegetated.

Comparison with the map of Lundin

The definition of classes in Lundin [23] is very different from the one presented in this work. It is therefore possible to compare these two maps. Grouping "Dry heath", "Mesic heath", "Alpine willow" allows them to be compared areas to the "Alpine tundra" class of Lundin. Similarly, our "Wetland" class is compared to the "Peatland" class of Lundin. The classes "Human infrastructure" and "Non vegetated" correspond to road, railway and building. The latter class is much more

Preprints (www.preprints.org) | NOT PEER-REVIEWED | Posted: 20 April 2023 doi:10.20944/preprints202304.0653.v1

represented on the Lundin map (Tables 10 and 11). The differences are related to a larger road and railway footprint, which does not affect the landscape dynamics. This observation shows the satisfactory overlay of the two maps.

Table 10. Distribution of land cover classes of [23] in the Stordalen watershed.

Class	Percentage
Rock	9
Alpine tundra	13
Peatland	11
Forest	51
Water	7
Non vegetated	9

Table 11. Distribution of land cover classes of our classification in the Stordalen watershed. The shadow class is not taken in account.

Class	Percentage
Rock	5
Dry heath/Mesic heath	9
Wetland	19
Alpine willow	2
Mountain birch	56
Water	7
Human infrastructure	2

The change matrix (Table 12) shows that the "Rock" class is also more represented on the map of Lundin, which covers twice as much space. The areas of this class that are not classified as rock for our map are located in the south of the map (Figure 4). They are contiguous to the “Rock” areas of our map. It is also possible that there has been a forest expansion between 2008 and 2002 in this area. Indeed, the forest has grown between 2008 and 2022. It has gained some space in all land cover categories. Furthermore, some areas of “Peatland” appear to be transformed into “Wetland” but Lundin [23] indicate "Peatlands were subdivided into wet areas (fen) and dry areas (bog) proportionally to what was found by Malmer et al. (2005)". It is therefore not possible to draw a conclusion from this observation. In summary, it is possible to compare our map with the map of Lundin after a semantic analysis of the categories. The main differences between the two maps concerns the south of the Stordalen watershed where Alpine toundra and forest are intermixed. The forest seems to have taken over areas previously occupied by tundra.

Table 12. Change matrix comparing our classification to the Lundin map [23]. Each column corresponds to the percentage of pixels of a class obtained by our classification in function of the Lundin classes. The shadow class is not taken in account.

		Our classification						
Lundin map		Rock	Dry heath / Mesic heath	Wetland	Alpine willow	Mountain birch	Water	Human infrastructure
	Rock	40	26	8	27	4	4	5
	Alpine tundra	27	26	12	28	11	4	8
	Peatland	3	10	30	6	7	8	7

Preprints (www.preprints.org) | NOT PEER-REVIEWED | Posted: 20 April 2023 doi:10.20944/preprints202304.0653.v1

Forest	16	27	37	25	66	34	28
Water	4	3	6	4	4	42	6
Non vegetated	10	8	7	10	8	8	46

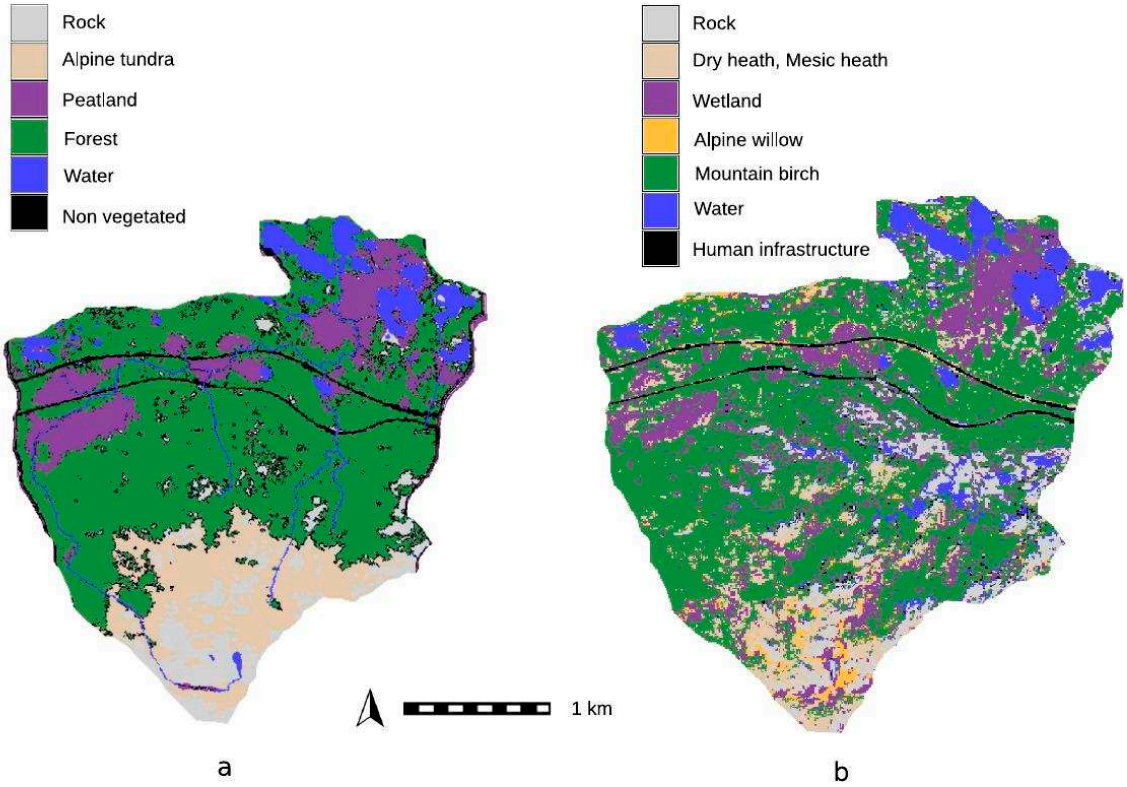

Figure 4. Land cover map by Lundin [23] (a) and our reclassified map (2022) (b) in the Stordalen watershed.

4. Discussion

The methodology implemented requires little sampling effort to quickly obtain a land cover map. This operation is feasible every year to monitor the evolution of land use. These results are particularly important in a region subject to climate change which is currently undergoing major upheaval.

The results of the Sentinel-2 image classification show a structuring of the landscape as a function of elevation, with different vegetation level along with altitude [39]. In the Miellajokka and Stordalen catchments, three levels are present. The subalpine level (< 600 m) is mainly occupied by "Mountain birch" formations. The alpine level [600 m , 1100 m] is characterized by "Dry heath", "Mesic heath" and "Alpine willow". This level could be split into two sub-levels according to the respective abundance of "Moutain birch" at lower altitude and "Rock" at upper altitude. The upper level, the nival level (> 1100 m), is only composed of rock.

Comparison between past and present vegetation maps is made difficult by the lack of a common typology field survey protocols. Nevertheless, It was possible to see a change in the landscape between 2008 and 2022. The analysis of the map of Lundin [23] and the one presented in this work would show an extension of the forest on the tundra towards the south (i.e., toward higher elevations) during the 2008-2022 period. This finding is in agreement with the map of Reese [11] which shows also a slight expansion of forest between 2011 and 2022 in the same direction. This trend could be a consequence of the on-going climate warming.

The proximity of the Abisko observation station makes the Meillajokka and Stordalen watersheds a privileged study area for the evolution of landscapes in the Arctic zone, in particular the thawing of the permafrost at high altitudes which is attested. This monitoring requires annual

surveys according to a unified protocol in terms of sampling effort, definition of classes and method of recording the surveys to monitor the evolution of this region subject to climate change.

Author Contributions: Conceptualization, Y. Auda and L. Orgogozo; methodology, Y. Auda and L. Orgogozo; software, Y. Auda; validation, Y. Auda, E. Lundin, J. Gustafsson, O.S. Pokrovsky, S. Cazaurang and L. Orgogozo; writing—original draft preparation, Y. Auda and L. Orgogozo; investigation, Y. Auda, L. Orgogozo and S. Cazaurang; writing—review and editing, Y. Auda, E. Lundin, J. Gustafsson, O.S. Pokrovsky, S. Cazaurang and L. Orgogozo; project administration, L. Orgogozo; funding acquisition, L. Orgogozo. All authors have read and agreed to the published version of the manuscript.

Acknowledgments: This work has been funded by the French Research Agency ANR (grant n ◦ ANR-19 CE46-0003-01), O.S. Pokrovsky was partially supported by the TSU Development Programme "Priority-2030". The authors would like to thank Reiner Giesler and Emily Pickering Pedersen for their help for preparing the field work.

References

1. Walvoord, M.; Kurylyk B. Hydrologic Impacts of Thawing Permafrost—A Review. Vadose Zone J. 2016, 15,6 ;. https://doi.org/10.2136 /vzj2016.01.0010
2. Meyer, G.; Humphreys, E.R.; Melton, J.R.; Cannon, A.J.; Lafleur, P.M. Simulating shrubs and their energy and carbon dioxide fluxes in Canada's Low Arctic with the Canadian Land Surface Scheme Including Biogeochemical Cycles (CLASSIC). Biogeosciences 2021, 18, 3263–3283;. https://doi.org/10.5194/bg-18-3263-2021
3. Jones, B.J.; Grosse, G.; Farquharson, L.M.; Roy-Léveillée, P.; Veremeeva, A.; Kanevskiy, M.Z.; Gaglioti, B.V.; Breen, A.L; Parsekian, A.D.; Ulrich, M.; Hinkel, K.M. Lake and drained lake basin systems in lowland permafrost regions. Nat. Rev. Earth Environ. 2022, 3, 85–98;. https://doi.org/10.1038/s43017-021-00238-9
4. Cable, W.L.; Romanovsky, V.E.; Jorgenson, M.T. Scaling-up permafrost thermal measurements in western Alaska using an ecotype approach. The Cryosphere, 2016;. https://doi.org/10, 2517–2532; DOI:10.5194/tc-10-2517-2016
5. Douglas, T.A.; Zhang, C., Machine learning analyses of remote sensing measurements establish strong relationships between vegetation and snow depth in the boreal forest of Interior Alaska. Environ. Res. Lett. 2021, 16 065014;. https://doi.org/10.1088/1748-9326/ac04d8
6. Zhang, Y.; Lantz, T.C.; Touzi, R.; Feng, W.; Kokelj, S.V. Landscape-scale variations in near-surface soil temperature and active-layer thickness: Implications for high-resolution permafrost mapping. Permafrost and Periglac Process. 2021, 32, 4, 627–640;. https://doi.org/10.1002/ppp.2104
7. Heijmans, M.M.P.D.; Magnússon, R.Í.; Lara, M.J.; Frost, G.V.; Myers-Smith, I.; van Huissteden, J.; Jorgenson, Fedorov, N.A.; Epstein, H.E.; Lawrence, D.M.; Limpens J. Tundra vegetation change and impacts on permafrost. Nat. Rev. Earth Environ. 2022, 3, 68–84;. https://doi.org/10.1038/s43017-021-00233-0
8. Bagard, M.-L.; Schmitt, A.-D.; Chabaux, F.; Pokrovsky, O.S.; Viers, J.; Stille, P.; Labolle, F.; Prokushkin, A. Biogeochemistry of stable Ca and radiogenic Sr isotopes in a larch-covered permafrost-dominated watershed of Central Siberia. Geochimica et Cosmochimica Acta 2013, 114, 169–187;. https://doi.org/10.1016/j.gca.2013.03.038
9. Orgogozo, L.; Prokushkin, A.S.; Pokrovsky, O.S.; Grenier, C.; Quintard, M.; Viers, J.; Audry, S. Water and energy transfer modeling in a permafrost-dominated, forested catchment of Central Siberia: The key rôle of rooting depth. Permafr. Periglac. Process. 2019, 30 75–89;. https://doi.org/10.1002/ppp.1995
10. Bartsch, A.; Höfler, A.; Kroisleitner, C.; Trofaier, A.M. Land Cover Mapping in Northern High Latitude Permafrost Regions with Satellite Data: Achievements and Remaining Challenges. Remote Sens. 2016, 8, 979;. https://doi.org/10.3390/rs8120979
11. Reese, H.; Nyström, M.; Nordkvist, K.; Olsson, H. Combining airborne laser scanning data and optical satellite data for classification of alpine vegetation. International Journal of Applied Earth Observation and Geoinformation 2014, 27, 81–90;. https://doi.org/10.1016/j.jag.2013.05.003
12. Greaves, H.E.; Eitel, J.U.H; Vierling, L.A.; Boelman, N.T.; Griffin, K.L.; Magney T.S.; Prager C.M. 20 cm resolution mapping of tundra vegetation communities provides an ecological baseline for important research areas in a changing Arctic environment. Environ. Res. Commun. 2019, 1;. https://doi.org/10, 10.1088/2515-7620/ab4a85
13. Langford, Z.L.; Kumar, J.; Hoffman, F.M.; Breen, A.L.; Iversen, C.M. Arctic Vegetation Mapping Using Unsupervised Training Datasets and Convolutional Neural Networks. Remote Sens. 2019, 11, 69;. https://doi.org/10.3390/rs11010069
14. Beamish, A.; Raynolds, M.K.; Epstein, H.; Frost, G.V.; Macander, M.J.; Bergstedt, H.; Bartsch, A.; Kruse, S.; Miles, V.; Tanis, C.M.; Heim, B.; Fuchs, M.; Chabrillat, S.; Shevtsova, I.; Verdonen, M.; Wagner ,J. 2020.

Recent trends and remaining challenges for optical remote sensing of Arctic tundra vegetation: A review and outlook. Remote Sens. Environ. 2020, 246, 111872;. https://doi.org/10.1016/j.rse.2020.111872
15. Rudd, D.A.; Karami, M.; Fensholt, R. Towards High-Resolution Land-Cover Classification of Greenland: A Case Study Covering Kobbefjord, Disko and Zackenberg. Remote Sens. 2021, 13, 3559;. https://doi.org/10.3390/rs13183559
16. IPCC, 2019. Summary for Policymakers. In IPCC Special Report on the Ocean and Cryosphere in a Changing Climate [H.O. Pörtner, D.C. Roberts, V. Masson-Delmotte, P. Zhai, M. Tignor, E. Poloczanska, K. Mintenbeck, M. Nicolai, A. Okem, J. Petzold, B. Rama, N. Weyer (eds.). https://www.ipcc.ch/site/assets/uploads/sites/3/2019/12/SROCC_FullReport_FINAL.pdf (accessed on 12 April 2023)
17. Patzner, M.S.; Logan, M.; McKenna, A.M.; Young R.B.; Zhou, Z.; Joss, H.; Mueller, C.W.; Carmen, H.; Scholten, T.; Straub, D; Kleindienst, S.; Borch, T.; Kappler A.; Bryce C. Microbial iron cycling during palsa hillslope collapse promotes greenhouse gas emissions before complete permafrost thaw. Commun. Earth Environ. 2022, 3, 76;. https://doi.org/10.1038/s43247-022-00407-8
18. Loranty, M.L.; Abbott, B.W.; Blok, D.; Douglas, T.A.; Epstein, H.E.; Forbes, B.C.; Jones, B.M.; Kholodov, A.L.; Kropp, H.; Malhotra, A.; Mamet, S.D.; Myers-Smith, I.H.; Natali, S.M.; O'Donnell, J.A.; Phoenix, G.K.; Rocha, A.V.; Sonnentag, O.; Tape, K.D.; Walker, D.A. Reviews and syntheses: Changing ecosystem influences on soil thermal regimes in northern high-latitude permafrost regions. Biogeosciences 2018, 15, 5287–5313;. https://doi.org/10.5194/bg-15-5287-2018
19. Malmer, N.; Johansson, T.; Olsrud, M.; Christensen, T.R. Vegetation, climatic changes and net carbon sequestration in a North-Scandinavian subarctic mire over 30 years. Global Change Biology 2005, 11, 1895–1909;. https://doi.org/10.1111/j.1365-2486.2005.01042.x
20. Tang, J.; Miller, P.A.; Persson, A.; Olefeldt, D.; Pilesjö, P.; Heliasz, M.; Jackowicz-Korczynski, M.; Yang, Z.; Smith, B.; Callaghan, T.V.; Christensen, T.R., 2015. Carbon budget estimation of a subarctic catchment using a dynamic ecosystem model at high spatial resolution. Biogeosciences 2015, 12,9, 2791-2808;. https://doi.org/10.5194/bg-12-2791-2015
21. Giesler, R.; Lyon, S.W.; Mörth, C.-M.; Karlsson, J.; Karlsson, E.M.; Jantze, E.J.; Destouni, G.; Humborg, C.; 2014. Catchment-scale dissolved carbon concentrations and export estimates across six subarctic streams in northern Sweden. Biogeosciences 2014, 11, 525–537.
22. Lundin, E.J.; Giesler, R.; Persson, A.; Thompson, M.S.; Karlsson, J. Integrating carbon emissions from lakes and streams in a subarctic catchment. JGR Biogeosciences 2013, 118, 1–8;. https://doi.org/10.1002/jgrg.20092
23. Lundin, E.J.; Klaminder, J.; Giesler, R.; Persson, A.; Olefeldt, D.; Heliasz, M.; Christensen, T.R.; Karlsson, J. Is the subarctic landscape still a carbon sink? Evidence from a detailed catchment balance. Geophys. Res. Lett. 2016 , 43, 1988–1995;. https://doi.org/10.1002/2015GL066970.
24. Mzobe, P.; Berggren, M.i; Pilesjö, P.; Lundin, E.; Olefeldt, D.; Roulet, N.T.; Persson, A. Dissolved organic carbon in streams within a subarctic catchment analysed using a GIS/remote sensing approach. PLOS ONE 2018, 13, 7, e0199608;. https://doi.org/10.1371/journal.pone.0199608
25. Mzobe, P.; Yan, Y.; Berggren, M.; Roulet, N.T.; Persson, A. Morphometric Control on Dissolved Organic Carbon in Subarctic Streams. Journal of Geophysical Research: Biogeosciences 2020, 125, e2019JG005348;. https://doi.org/10.1029/2019JG005348
26. Hardisky, M.A.; Kiemas, V.; Daiber, F.C. Remote sensing salt marsh biomass and stress detection. Adv. Space Res. 1983, 2, 8, 219-229.
27. Gao, B.C. NDWI - a normalized difference water index for remote sensing of vegetationfor liquid water from space. Remote Sens. Environ. 1996, 58, 257-266.
28. Ostadabbas, H.; Weippert, H.; & Behr, F. J. Using the synergy of qfield for collecting data on-site and qgis for interactive map creation by alkis® data extraction and implementation in postgresql for urban planning processes. Int. Arch. Photogramm. Remote Sens. Spatial Inf. Sci. 2020, 679-683;. https://doi.org/10.5194/isprs-archives-XLIII-B4-2020-679-2020
29. Breiman, L. Statistical Modeling: The Two Cultures, Statistical Science, 2001, 16, 3, 199-231.
30. Neteler, M.; Mitasova, H. 2008. Open Source GIS: A GRASS GIS Approach, 3rd ed. Springer, New York.
31. Ermakov, N.; Shaulo, D.; Maltseva T. The class Mulgedio-Aconitetea in Siberia. Phytocoenologia 2000, 30, 2 145-192.
32. Hjort, J.; Luoto M. 2009. Interaction of geomorphic and ecologic features across altitudinal zones in a subarctic landscape. Geomorphology 2009, 112, 324-333.
33. Sieg, B.; Drees B.; Hasse, T. High-altitude vegetation of continental West Greenland. Phytocoenologia 2019, 39,1, 27–50
34. Sundqvist, M.; Giesler, R.; Graae, B.J.; Wallander, H.; Fogelberg, E.; Wardle, D.A. Interactive effects of vegetation type and elevation on aboveground and belowground properties in a subarctic tundra. Oikos 2011, 120, 128–142;. https://doi.org/10.1111/j.1600-0706.2010.18811.x

35. Sundqvist, M.; Liu, Z.; Giesler, R.; Wardle, D.A. Plant and microbial responses to nitrogen and phosphorus addition across an elevational gradient in subarctic tundra. Ecology 2014, 95, 7 1819–1835;. https://doi.org/10.1890/13-0869.1
36. Lyon, S.W.; Ploum, S.W.; van der Velde, Y.; Rocher-Ros, G.; Mörth, C.-M.; Giesler, R. Lessons learned from monitoring the stable water isotopic variability in precipitation and streamflow across a snow-dominated subarctic catchment. Arctic, Antarctic, and Alpine Research 2018, 50, 1, e1454778;. https://doi.org/10.1080/15230430.2018.1454778
37. Rocher-Ros, G.; Sponseller, R.A.; Lidberg, W.; Mörth, C.-M.; Giesler, R. Landscape process domains drive patterns of CO2 evasion from river networks. Limnol Oceanogr Lett, 2019, 4, 87-95;. https://doi.org/10.1002/lol2.10108
38. Borgelt, J. Terrestrial respiration across tundra vegetation types - Implications for arctic carbon modelling. Master Degree report of Umeå University. 2017.
39. Troll, C. High mountain belts between the polar caps and the equator: their definition and lower limit. Arctic and Alpine Research 1973, 5, 3, A19-A27